Analyses of Global Monthly Precipitation Using Gauge Observations, Satellite Estimates, and Numerical Model Predictions

PINGPING XIE* AND PHILLIP A. ARKIN

National Center for Environmental Prediction, National Oceanic and Atmospheric Administration, Washington, D.C.

(Manuscript received 10 February 1995, in final form 18 September 1995)

ABSTRACT

An algorithm is developed to construct global gridded fields of monthly precipitation by merging estimates from five sources of information with different characteristics, including gauge-based monthly analyses from the Global Precipitation Climatology Centre, three types of satellite estimates [the infrared-based GOES Precipitation Index, the microwave (MW) scattering-based Grody, and the MW emission-based Chang estimates], and predictions produced by the operational forecast model of the European Centre for Medium-Range Weather Forecasts. A two-step strategy is used to: 1) reduce the random error found in the individual sources and 2) reduce the bias of the combined analysis. First, the three satellite-based estimates and the model predictions are combined linearly based on a maximum likelihood estimate, in which the weighting coefficients are inversely proportional to the squares of the individual random errors determined by comparison with gauge observations and subjective assumptions. This combined analysis is then blended with an analysis based on gauge observations using a method that presumes that the bias of the gauge-based field is small where sufficient gauges are available and that the gradient of the precipitation field is best represented by the combination of satellite estimates and model predictions elsewhere. The algorithm is applied to produce monthly precipitation analyses for an 18-month period from July 1987 to December 1988. Results showed substantial improvements of the merged analysis relative to the individual sources in describing the global precipitation field. The large-scale spatial patterns, both in the Tropics and the extratropics, are well represented with reasonable amplitudes. Both the random error and the bias have been reduced compared to the individual data sources, and the merged analysis appears to be of reasonable quality everywhere. However, the actual quality of the merged analysis depends strongly on our uncertain and incomplete knowledge of the error structures of the individual data sources.

1. Introduction

The spatial and temporal distribution of large-scale precipitation is critical in determining the general circulation of the atmosphere and the global climate. Scientists attempting to simulate the behavior of the global climate system must compare the precipitation fields produced by their simulations with observed fields. Those wishing to understand the interannual variability in the general circulation related to variations in tropical sea surface temperature require accurate observations of the associated large-scale precipitation variations.

Despite these requirements, the distribution of global precipitation is not well documented, both because of its large spatial and temporal variability and the lack of a comprehensive observing system. The principal existing sources of information on climatic-scale precipitation are gauge observations and estimates inferred from satellite data, each of which has advantages as well as shortcomings (Barrett and Martin 1981; Arkin and Ardanuy 1989). Generally speaking, raingauge observations yield relatively accurate point measurements of precipitation but suffer from sampling error in representing areal means and are not available over most oceanic and unpopulated land areas. Infrared (IR) and passive microwave (MW) satellite observations can be used to derive estimates of large-scale precipitation over much of the globe, but these estimates are characterized by nonnegligible bias and random error associated with inadequate sampling, algorithm errors, and the indirect nature of the physical relationship between precipitation and the observations.

In order to quantitatively understand the capabilities of existing data sources and algorithms, Xie and Arkin (1995) conducted a comprehensive examination of several existing sources of climatic-scale precipitation. By intercomparing three sets of gauge observations (GPCC, CAMS, and Morrissey atoll data) and eight different satellite estimates (one IR-based, three MW scattering-based, and four MW emission-based) of monthly precipitation for a 3-yr period (July 1987–

* RDC Research Scientist.

Corresponding author address: Dr. Pingping Xie, National Center for Environmental Prediction, W/NMC, NOAA/NWS, Washington, D.C., 20233.
e-mail: xping@sgi17.wwb.noaa.gov

June 1990), with two versions of long-term average precipitation (Jaeger 1976; Legates and Willmott, 1990), they found the following:

1) At least five gauges are needed to produce areally averaged monthly precipitation for grid areas of 2.5° × 2.5° latitude–longitude with an accuracy of 10%. At the present time, only 10% of the global land grid areas satisfy this requirement.

2) Different satellite estimates based on a given sort of observational data (IR, MW scattering, or MW emission) yield similar results relative to concurrent gauge observations (i.e., differences among MW-scattering estimates are small compared to their differences from MW-emission estimates). Estimates based on different sources vary significantly in their capability to represent precipitation in different seasons, of different latitudinal regions, and over different underlying surfaces.

3) Over tropical and subtropical areas, all satellite estimates show high correlation and stable bias over ocean when compared to atoll-based gauges, while over land they exhibit high pattern correlation but with large seasonally and regionally dependent bias. Over mid and high latitudes over land, where the IR-based and MW-emission-based estimates were not available, the MW-scattering-based estimates performed poorly in representing the spatial and temporal variability of precipitation, especially during the winter and early spring.

The intercomparison results have shown clearly that at least three major deficiencies exist in the individual sources of precipitation: 1) incomplete global coverage; 2) significant random error; and 3) nonnegligible systematic error (bias). It is therefore necessary to improve the quality of the individual data sources and to combine the different sources so as to take advantage of the strengths of each. While further improvements of the individual sources are essential, particularly over mid and high latitudes where no single source yields satisfactory results in all seasons, an appropriate combination of the estimates from the different sources might provide us with complete gridded fields, which we will call analyses, of global monthly precipitation with quality everywhere equal to or better than that of each of the individual components.

In this paper, we present a new algorithm to merge various kinds of monthly precipitation datasets into global gridded fields of areally averaged precipitation. Gauge observations, satellite estimates from IR, MW-scattering and MW-emission observations, and predictions from numerical weather forecast models are used to ensure complete global coverage. A two-step strategy is used to reduce the random error found in the five individual sources and to reduce the bias of the combined analysis. First, the three satellite-based estimates and the model predictions are combined linearly, based on a maximum likelihood estimate in which the weighting coefficients are inversely proportional to the squares of the individual random errors determined by comparison with gauge observations and subjective assumptions. This combined analysis is then blended with an analysis based on gauge observations using a method that presumes that the bias of the gauge-based field is zero where sufficient gauges are available and that the gradient of the precipitation field is best represented by the combination of satellite estimates and model predictions elsewhere. Section 2 will describe the methodology and the individual data sources used in the merging procedure, and sections 3, 4, and 5 will present the methods for combining and blending the individual sources and for defining the error of the merged analysis. Section 6 will show some applications of the algorithm, and a summary and conclusions will be given in section 7. These sections are arranged so that potential users of the resulting global analyses can understand the procedure conceptually from sections 1), 2), 6), and 7), while readers interested in the technical details of the algorithm can find them in sections 3), 4), and 5).

2. Methodology and data

a. Merging methodology

Merging of precipitation observations from different sources has been demonstrated to be a powerful means for improving the overall measurement quality. Early efforts have focused on combining point measurements from gauges with digitized radar observations on regional scales and have led to successful operational applications in Japan (Takemura et al. 1984) and in the United Kingdom (Browning 1979; Conway 1987). Similar work is underway to merge gauge data with WSR-88D observations in the United States (Krajewski 1987).

Recently, work has begun on combining different satellite estimates. The pioneering work in this area is reported by Adler et al. (1993, 1994). They assume that their MW-scattering-based estimates give accurate instantaneous rain rate but with poor sampling in space and time and that the IR estimates [GOES Precipitation Index, GPI, of Arkin and Meisner (1987)] provide good coverage in space and frequent sampling in time but with significant systematic error. They then calculate the ratio between the MW and IR estimates when both are available and use the ratio to adjust the IR estimates. An application of the technique has shown some success in estimating warm season precipitation over Japan (Negri and Adler 1993).

These combined satellite estimates have been used with other data to construct complete global precipitation analyses. Assuming that both the analyses based on gauge observations produced by the Global Precipitation Climatology Centre (GPCC 1992, 1993) and the adjusted satellite estimates of Adler et al. (1994) are unbiased, Huffman et al. (1995) combined the two

kinds of sources linearly using optimal coefficients that are inversely proportional to the square of the errors of the individual sources. Grid areas with no observations of either sort were filled with operational numerical weather forecast model predictions from the European Centre for Medium-Range Weather Forecasts (ECMWF) (Arpe 1991). These efforts have succeeded in producing the first complete global depictions of monthly precipitation distribution from multiple sources of information, including gauge observations, satellite-derived estimates, and model predictions, together with estimates of the spatial distribution of relative error.

Some improvements upon the Huffman et al. (1995) algorithm are possible. First, the use of only two kinds of data sources (the gauge-based analysis and the MW-adjusted IR estimates) limits the capability of the algorithm to reduce the individual random errors that are significant for satellite estimates, especially over extratropical areas (Xie and Arkin 1995). Second, the linear combination of the different sources used in the algorithm is not able to remove biases present in the component sources. As revealed by Morrissey and Greene (1993) and Xie and Arkin (1995), all of the satellite estimates examined show nonnegligible bias when compared with concurrent in situ observations. Finally, the manner in which they use model predictions to fill the gaps of the combined analysis results in discontinuous borders within the analysis due to substantial biases between the model predictions and the other sources.

We have designed and developed an algorithm to produce global monthly precipitation analyses by merging several kinds of different data sources, based upon the knowledge obtained through the intercomparison of Xie and Arkin (1995). The merging algorithm begins with the selection of the individual data sources. As different precipitation products (analysis–estimates) based upon the same observational data sources provide basically similar performance in depicting spatial and temporal variations, and inclusion of additional data sources with the same characteristics is unlikely to improve the merged analysis significantly (Xie and Arkin 1995), only one of each kind of individual precipitation product is selected from each of the four categories of different data sources: 1) gauge observations; 2) satellite IR-based estimates; 3) satellite MW-scattering-based estimates; and 4) satellite MW-emission-based estimates. As none of these data sources provides complete coverage of monthly precipitation over mid and high latitudes, numerical weather forecast model predictions are included as the fifth individual source to ensure complete global coverage.

The two steps of the merging algorithm are designed to first reduce the random error and then to reduce the bias. First, the three categories of satellite estimates and the model predictions are linearly combined to minimize the random error. The linear combination coefficients are determined by maximum likelihood estimation and are inversely proportional to the square of the local random errors of the individual sources. These errors are defined for each land grid area by comparison with the GPCC gauge analysis over the surrounding area and for oceanic grid areas by comparison with the atoll gauge observations (Morrissey and Greene 1991) over the Tropics and subjective extension to the extratropics.

The output of the first step contains significant bias passed through from the individual sources, and so the purpose of the second step is to reduce that bias. For this purpose, we make the assumption that the gauge-based analysis is unbiased in regions where sufficient observations are available. It is well known that gauge observations in general are biased (Sevruk 1982; Legates and Willmott 1990), as are analyses of areally averaged precipitation based on gauge observations. These biases have a variety of sources, including gauge type, maintenance and siting, and spatial sampling. Estimation and correction of these biases in a global dataset is exceedingly difficult (Schneider et al. 1993; Rudolf et al. 1994). However, it is thought that they are small compared to the biases in the satellite estimates and model forecasts. Therefore, in this paper, we have assumed that the bias of the gauge-based analysis is zero where the sampling of gauges is adequate. This provides a convenient method by which the merged analysis can be improved in the likely event that improved gauge-based analyses become available.

Over global land areas, the combined analysis and the gauge analysis are blended using the method of Reynolds (1988), in which the relative distribution, or "shape," of the blended analysis is determined by the combined analysis, while the amplitude is defined by the gauge analysis at grid areas with "enough" gauges. The definition of enough, of course, requires investigation and is discussed below. Over oceanic areas, the bias remaining in the combined analysis is removed by comparing with concurrent atoll gauge observations over the Tropics, again presuming the spatial mean of the gauge observations to be unbiased, and by simple and somewhat subjective extrapolation of the bias structure of the combined analysis into higher latitudes.

Our algorithm in its present form contains two significant defects: it takes no account of the horizontal correlation present in most of the components used, and it linearly combines biased estimates before removing the biases. While the horizontal spatial correlations contained within individual datasets can be one of the most useful sources of information for improving the quality of analyzed fields (Daley 1991), they are not used in our present algorithm in which the random errors are reduced through linear combination for individual grid areas. We will attempt to modify our algorithm to take advantage of the information provided by horizontal correlations in the future. In general, ob-

jective analysis techniques (e.g., Krajewski 1992) are applied to the optimal linear combination of *unbiased* component estimates. We have chosen to combine *biased* estimates because the method we use to remove bias over land [based on that of Reynolds (1988)] requires a spatially complete field with reasonable pattern agreement to the "true" precipitation field (i.e., modest random error). However, that requirement cannot be satisfied in general by any of the individual satellite estimates and model predictions. We create the necessary spatially complete field by defining the individual random errors as the root-mean-square differences between the GPCC gauge analysis and the individual sources after the bias is removed locally (see section 3 for details). While this does not strictly satisfy the theoretical requirements of the maximum likelihood estimation procedure, our verification against withheld data (see sections 3 and 4) shows that the algorithm succeeds in reducing both random error and bias.

The final product of the merging algorithm has complete global coverage of monthly precipitation with better quality than any of the five individual sources used. The characteristics of the various components of the algorithm are investigated in sections 3 and 4. For convenience, we will refer to the first step as combining, the second step as blending, and the entire process as merging in the following discussions.

b. *Individual data sources*

Our merging algorithm is intended to permit the combination of a raingauge-based analysis of precipitation with a weighted average of satellite-derived IR-, MW-scattering-, and MW-emission-based estimates and numerical weather forecast model predictions. It is used in this study to produce analyses of global monthly precipitation on a 2.5° × 2.5° latitude–longitude grid for an 18-month period from July 1987 to December 1988. The individual data sources used in this study are the GPCC gauge analysis [supplemented by the atoll gauge observations compiled by Morrissey and Greene (1991) over the ocean], the GOES Precipitation Index (GPI) (Arkin and Meisner 1987), the Grody MW-scattering index (Ferraro et al. 1994), the Chang MW-emission estimates (Wilheit et al. 1991), and the ECMWF precipitation predictions. Table 1 presents a brief description of the five types of data source.

The GPCC dataset consists of a 2.5° × 2.5° gridded analysis of monthly precipitation created by statistically interpolating quality-controlled gauge observations from about 6700 stations worldwide (GPCC 1992; 1993). In addition to the analyzed value, the number of gauges in each grid area is also available and is used in this study as an indicator of the data quality. As the GPCC analysis does not cover the global oceanic areas, the atoll gauge rainfall dataset edited by Morrissey and Greene (1991) is used to define the error structure of the individual satellite estimates and model predictions over the tropical Pacific Ocean. The atoll gauge dataset comprises station observations of monthly precipitation from about 100 gauges located on small islands without high terrain. Monthly mean precipitation for 2.5° × 2.5° latitude–longitude areas is calculated for all grid areas with at least one gauge. As shown in Fig. 1 of Xie and Arkin (1995), the atoll gauges are mainly located in the western Pacific along a northwest to southeast axis extending from 10°N and 140°E across the equator to 20°S and 140°W. The number of gauges in each grid area varies from 1 to 8, with an average of 2–3.

TABLE 1. Individual data sources.

Category	Technique	Coverage
Gauge	GPCC/atoll	Land–atoll
IR	GPI	40°S–40°N
MW scattering	Grody	Global land–ocean
MW emission	Chang	Global ocean
Model	ECMWF	Global land–ocean

The IR-based GPI estimates climatic-scale precipitation from the fractional coverage of clouds colder than 235 K in geostationary imagery using an empirical linear equation obtained from observations during the GATE (Arkin 1979; Richards and Arkin 1981). The GPI estimates used in this study have been produced by the Global Precipitation Climatology Project (GPCP) (Arkin and Xie 1994) based on eight observations each day where geostationary satellite data were available and four each day from polar-orbiting satellites elsewhere. The estimates are available from 40°S to 40°N over both land and ocean. Verification over Japan, the United States, China, and the tropical Pacific has shown that the GPI is able to estimate the pattern of convective rainfall in the Tropics and, during the warm season, in some midlatitude regions, with only a small bias over the tropical ocean but with a large positive bias over land (Janowiak 1992; Arkin and Xie 1994; Arkin et al. 1994; Xie and Arkin 1995).

The Grody MW scattering-based estimates (Grody 1991; Ferraro et al. 1994) are derived from the scattering signal of ice particles observed from the Special Sensor Microwave/Imager (SSM/I) on the Defense Meteorological Satellite Program (DMSP) satellites in two steps. First, nonraining and indeterminate pixels are eliminated by a variety of tests based on the data from various channels. A scattering Index (SI) is then computed from the brightness temperatures at 19V, 22V and 85V GHz channels and is converted into a rain rate using an empirical relation derived from radar data over Japan. The Grody estimates are available over all land and oceanic areas for all seasons, although surface snow or ice prevents successful estimation in parts of the high latitudes. While the Grody estimates are based on observations related more directly to the precipitation than those on which the GPI is based, they

are not capable of detecting precipitation not associated with ice and are therefore most accurate in estimating deep convective precipitation. Comparisons with surface observations have shown that the Grody estimates have comparable skill to the IR-based GPI in representing precipitation over tropical and extratropical areas (Dodge 1994; Xie and Arkin 1995). During the period of this study, one SSM/I was available, yielding between 1 and 2 observations at a given location in the Tropics each day.

The Chang MW emission-based estimates (Wilheit et al. 1991; Chiu et al. 1993) are constructed by retrieving precipitation information from thermal emission of liquid water as observed by the SSM/I. The histogram of a linear combination of the 19V and 22V GHz channels is computed from observations and from a radiative transfer model using various combinations of parameters for rain rates in the target area. The parameters that result in the histogram that best matches the observations are then used to calculate the rainfall estimates for the area. The Chang estimates used in this study are available over oceanic areas between 65°S and 65°N but are not available over land areas. These estimates are especially useful in depicting precipitation over oceanic areas with significant warm rain (not associated with large ice particles), for example, in the eastern Pacific intertropical convergence zone (ITCZ) during northern winter (Janowiak et al. 1995).

The GPCC provided the numerical weather forecast model predictions of global precipitation used in this study. They were obtained by accumulating operational 24-h forecasts for the period from 12 to 36 hours from initial time from the ECMWF T106 model for each month during the period. The 12–36-h forecasts were selected so as to minimize the so-called spinup effects, which can result in unrealistically large amplitudes in the early portion of the forecast period. The ECMWF monthly precipitation predictions are available for the entire globe, with better quality over mid and high latitudes, particularly in the Northern Hemisphere, where more reliable observations are available to define the initial conditions for the forecasts (Arpe 1991).

3. Combining of the satellite estimates and model predictions

a. Combining algorithm

Mathematically, we consider the combination of the three kinds of satellite estimates and the model predictions as a search for the most probable value C of areally averaged precipitation (maximum likelihood estimation; Daley 1991) given the four individual observations P_i. Assuming that 1) the observation error σ_i is random, unbiased, and normally distributed for each kind of observation P_i, and 2) the observation errors for different kinds of observations are independent, the maximum likelihood estimate of C is defined as

$$C = \Sigma W_i P_i, \tag{1}$$

where

$$W_i = \frac{\sigma_i^{-2}}{\Sigma \sigma_i^{-2}} \tag{2}$$

and the expected error variance of C is given by

$$\langle \epsilon^2 \rangle = [\Sigma \sigma_i^{-2}]^{-1}. \tag{3}$$

Thus, the maximum likelihood estimate of the precipitation at a given grid area is a linear combination of the individual data sources (estimates or predictions), in which the combination coefficients are inversely proportional to the observation error variance of each source. Furthermore, because the expected error of the maximum likelihood estimate is always less than those for the individual sources, as shown in Eq. (3), the combining process based on Eqs. (1) and (2) should reduce the error of C relative to the individual sources.

In the present study, the basic assumptions of the method are not satisfied because the individual observations (estimates and predictions) contain both random and systematic (bias) errors whose distribution is unknown. In order to permit the practical application of this process, we define the observation errors in Eqs. (2) and (3) as the random errors of the individual sources following empirical removal of the "local" bias. This bias removal applies only to the calculation of the random errors; otherwise the bias of the individual sources is ignored at this stage and will therefore remain in the combined analysis C as a linear combination of the individual biases. The combining algorithm is thus composed of two major components: 1) definition of the random errors; and 2) linear combination of the four kinds of individual sources.

The differences in the availability of gauge observations make it necessary to use different methods to define the individual random errors for land and ocean areas. Over land areas, the GPCC precipitation analysis, which is available for each grid area, is used as a standard reference. First, the mean difference between the source field and the GPCC analysis is calculated for a 7×7 array of grid areas centered on the target grid area and subtracted from the source field over that array. The random error for each grid area for each individual source for each month is then defined as the root-mean difference between this modified source field and the GPCC analysis calculated on the same 7×7 array. The GPCC analysis values at all land grid areas are used in the computation, regardless of the number of gauges available. When the 7×7 array is not completely filled by the GPCC analysis (as happens near coastlines), the subset for which values are available is used. This process results in a well-defined estimate for the random error for each source for each land grid area. The accuracy of the estimated error is determined by the (unknown) errors in the GPCC anal-

ysis. However, we believe that this estimate is superior to one based entirely on sampling frequency or subjective judgements.

Over oceanic areas, where no complete spatial analysis exists because the available gauge observations are inadequate for satisfactory spatial and temporal coverage, the same process cannot be used. Instead, the random errors for the four individual sources are defined as the root-mean-square difference between the modified (by subtraction of the spatial mean difference between the original source field and the atoll gauges) source field and the concurrent atoll gauge precipitation observations of Morrissey and Greene (1991) over the tropical Pacific. These error values, as a percentage of the mean, are applied to all ocean grid areas in the deep Tropics. For higher latitudes, the relative error varies with latitude, season, and source. For the IR-based GPI and the MW-scattering-based Grody estimates, errors are known to be greater in regimes in which deep convective precipitation is less frequent (Xie and Arkin 1995). Thus we expect the relative error to increase smoothly poleward from the observationally determined values at the boundary of the Tropics to very large values at the polar limits of the utility of each. For this purpose, the boundary of the Tropics varies from 15° in the winter hemisphere to 25° in the summer hemisphere, and the poleward limits of utility are between 25° and 40° for the GPI and up to 90° for the Grody estimates. For the MW emission-based Chang estimates, the tropical error value is used for all latitudes, since the quality of the algorithm is not thought to depend much on the climatic regime. For the ECMWF model predictions, we estimate that the error decreases poleward, with values in high latitudes half those in the Tropics, due to the greater skill of the model in predicting precipitation from mid- and high-latitude cyclonic systems than from tropical convective systems.

The errors calculated from the source fields and the atoll data over the tropical Pacific, together with extrapolation based on the subjective assumptions described above, permit us to define oceanic random errors for each of the individual sources for each month. Figure 1 shows an example of the latitudinal profiles of the oceanic random errors obtained by this process for August 1987. Note that the errors are defined only where sufficient ocean area is found (thus the gap at 60°N) and where the individual source is available. Using these individual random errors for both the land and oceanic areas, the global distribution of the combined analysis C is constructed by calculating the maximum likelihood estimate from the four individual sources using Eqs. (1) and (2).

b. *Tests on synthetic data*

For any algorithm developed to extract meteorological information from observations, verification of feasibility and performance must precede practical application. This is generally done through comparison of the algorithm output with independent observations not included in the information used by the algorithm. In the estimation of precipitation from satellite observations, these independent observations (sometimes inaccurately called "ground truth") are often obtained from raingauges and/or radars (Arkin and Meisner 1987; Arkin and Xie 1994). In the combining algorithm described here, however, the spatial scale and the inclusion of all available gauge observations make such an examination for the whole target domain impossible. Application of the algorithm to synthetic datasets and analyses based on subsets of the available data and evaluated against unused observations are therefore used as validation.

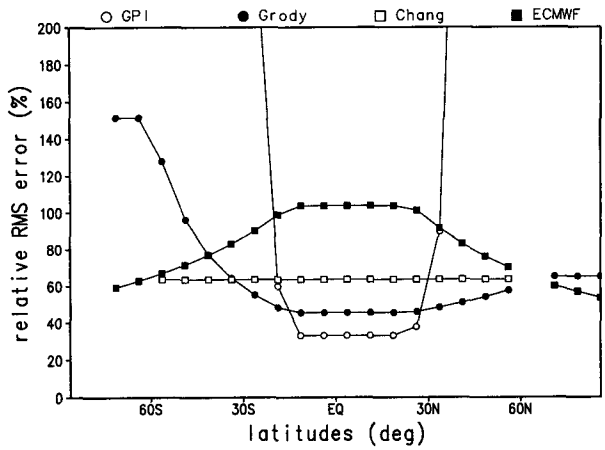

FIG. 1. Latitudinal profiles of the relative rms errors of the individual sources over oceans for August 1987.

Application of the algorithm to synthetic datasets with well-defined characteristics enables us to examine its performance under controlled circumstances. We begin by defining a "true," or target, precipitation field. Generally speaking, there are two ways in which this can be done. One is to generate the field by a numerical model that can accurately reproduce the details of the statistical and spatial structure of the precipitation field (Waymire et al. 1984; Bell 1987). The other is to use a high quality observed or analyzed field (Krajewski 1987). In this study, we choose the latter and use the final merged analysis based on observational data for the August 1987 as our "truth" field. Synthetic source fields with characteristics representative of the various satellite estimates, the model predictions, and the gauge-based analysis are then obtained by defining their spatial coverage (the percentage of the 2.5° latitude–longitude grid areas with values) and then adding bias and/or random error to the "truth" field. The omitted grid areas and the specific error values to add to any given grid area are derived from a uniformly distributed random variable, while the ranges for these

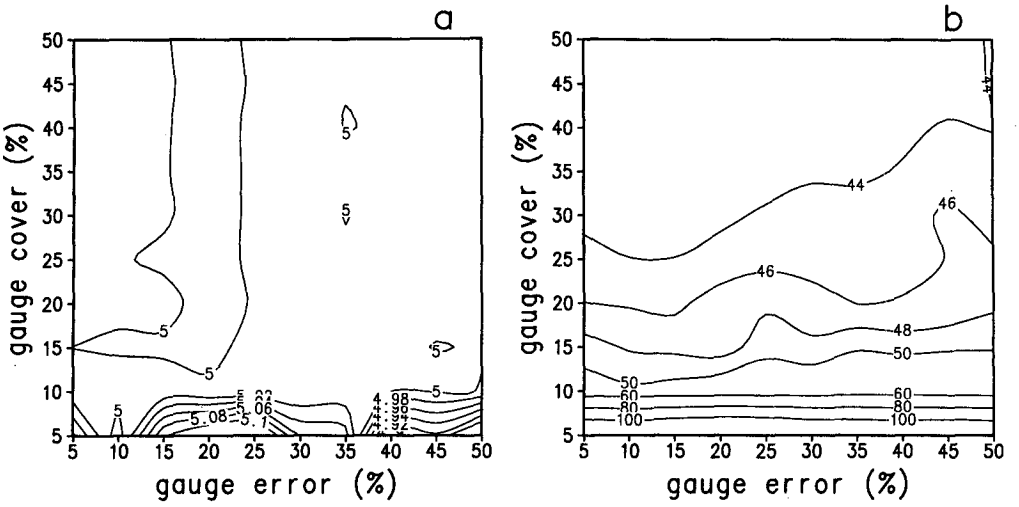

FIG. 2. Biases in millimeters per day (a) and relative rms errors in percent (b) between the target field (the merged analysis for August 1987) and the combined analyses obtained from simulated individual sources with bias of 5.0 mm day^{-1} and random error of 100% when the error structures are determined from simulated gauge data with various coverages and errors.

parameters are taken from observational studies (Xie and Arkin 1995). The algorithm is applied to the synthetic source fields and the merged product is compared to the "truth" field to determine the impact of varying coverages and errors. One advantage of this process is that it permits us to investigate the response of the algorithm to a variety of simplified situations that might exist in the real world but are difficult to isolate in actual observations. The spatial distribution of coverage and random error of the synthetic fields differs from the actual situation, in which both are regionally coherent (Xie and Arkin 1995). The assumption of globally uniform bias in the synthetic fields is also an oversimplification. Despite these deficiencies, we expect these simplified situations to provide us with insight into the response of the algorithm to the incompleteness and error of the actual gauge-based analysis and the individual sources.

The success of the initial combination stage of the algorithm depends largely on how accurately the error structures of the individual sources are defined by comparison with the gauge-based analysis over the surrounding area. We therefore begin by investigating the impact of varying spatial coverage and random errors in the gauge-based analysis on the product of the combining algorithm. Since the density of the gauge network varies greatly over global land areas and the random error of the gauge observations is strongly influenced by the network density, a total of 100 combinations of gauge fields are simulated, with both the spatial coverage and the random error ranging from 5% to 50% in interval of 5%. This range is representative of the GPCC global monthly precipitation analysis, in which the percentage coverage and the relative error of monthly precipitation are 45% and 30%–50% for grid areas with at least one gauge and 10% and 5%–10% for grid areas with at least five gauges, respectively (Xie and Arkin 1995). For simplicity, the bias of the gauge-based analysis is assumed to be zero here. Our algorithm is applied to combine these synthetic gauge-based analyses with synthetic "satellite/model" fields with random errors averaging 100% and uniform bias of 5 mm/day, representative of certain satellite estimates over tropical land areas (Xie and Arkin 1995), and the results are compared to the target field. The bias of the combined analyses that result remains approximately 5.0 mm day^{-1} for all combinations of gauge coverage and errors (Fig. 2a), while the random error decreases with increasing gauge coverage (Fig. 2b). These results show that sufficient coverage (>10%) of gauge observations is vital to the correct definition of the weighting coefficients and therefore to the effective reduction of the random error in the combined analysis, while random error in the gauge observations has no significant impact on the bias and random error in the combined analysis.

Next we wish to investigate the impact on the combined analysis of varying random errors in the "satellite/model" source fields. We again use a synthetic gauge-based analysis with coverages ranging from 5% to 50% and with a random error averaging 20%. Our synthetic source fields are given a uniform bias of 5 mm/day and mean random errors ranging from 20% to 200%. This range of random error includes the typical random errors of 50% and 100% for satellite estimates over tropical oceanic and land areas, as well as the 200% random error that has been observed over extratropical land areas in cold seasons for some satellite

estimates (Xie and Arkin 1995). Comparison between the target field and the resulting combined analyses shows that the biases of the synthetic sources (Fig. 3a) are essentially unchanged in the combined analyses. However, the random error of the combined analyses is reduced to about one-half of the error in the simulated sources when the gauge coverage is larger than 10%, in agreement with theoretical calculations based on Eq. (3), and increases rapidly with the decrease of gauge coverage below the 10% threshold.

c. *Validation*

Tests using synthetic data have helped us to understand the sensitivity of the combined analysis to the coverages and errors of the various sources of information used. Here we will try to evaluate the performance of the algorithm in combining actual fields of monthly satellite estimates, model predictions, and gauge-based analyses, whose coverages and error structures are not reflected perfectly in the simulations. In general application, our algorithm is intended to use all available information, and, therefore, no independent observations of precipitation exist to validate against. Clearly, comparisons of our analyzed field with the gauge-based analysis used would be meaningless. Therefore, we have used the algorithm to combine the four satellite/model sources using only a randomly selected 75% of land and atoll grid areas from the gauge-based analysis to determine the weights. The resulting combined analysis is then compared to the gauge-based analysis over the unused 25% of the grid areas. While this comparison is not against truly independent observations, since there is spatial autocorrelation in the monthly global precipitation field and since the analysis method used by the GPCC might have introduced spurious smoothing, we believe that this is the only means available to us to demonstrate that the combining and merging algorithms improve upon the individual sources.

The time series of the pattern correlation, bias, and relative root-mean-square (rms) error for the individual sources and the combined analysis for the tropical Pacific Ocean, tropical land areas (40°S–40°N), and extratropical land areas (40°–90°S; 40°–90°N) are shown in Figs. 4, 5, and 6, respectively. The same statistics for the whole 18-month period are shown in Table 2. The combined analysis in the tropical Pacific has statistics comparable to the individual sources (Fig. 4), several of which have relatively high skill in describing tropical precipitation (Xie and Arkin 1995). Large fluctuations are observed in the time series in this region, possibly because only nine independent grid areas were available for comparison. Over tropical (Fig. 5) and extratropical (Fig. 6) land areas, the combined analysis shows very stable statistics and reduced random error compared to those of the four individual sources. Overall, the random error has been reduced substantially relative to each of the original sources, while the correlation is generally higher. The bias remains as a combination of the individual biases.

4. Blending of the combined analysis and the gauge observations

a. *Blending algorithm*

Since the combined analysis contains bias passed through from the individual satellite estimates and model predictions, the second step of the merging al-

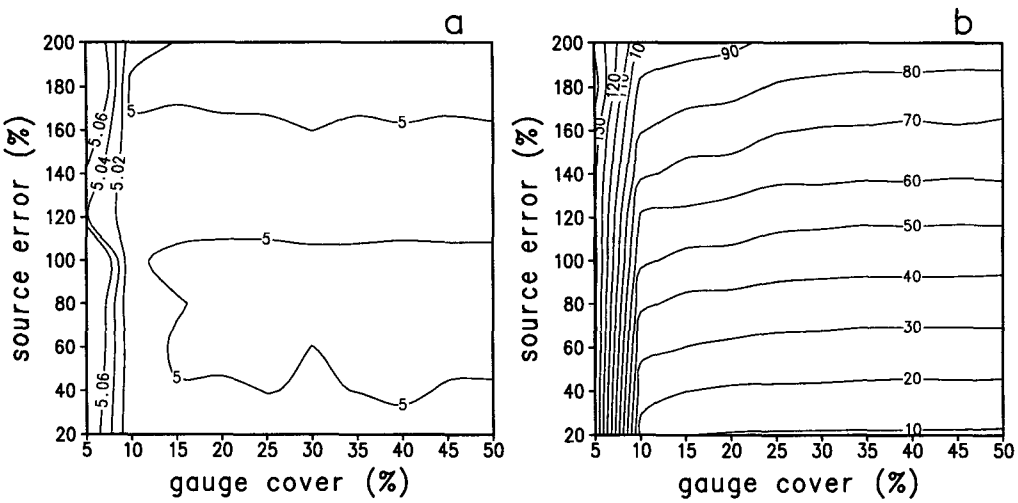

FIG. 3. Biases in millimeters per day (a) and relative rms errors in percent (b) between the target field (the merged analysis for August 1987) and the combined analyses obtained from simulated individual sources with bias of 5.0 mm day^{-1} and various random errors when the error structures are determined from simulated gauge data with various coverages and fixed random error of 20%.

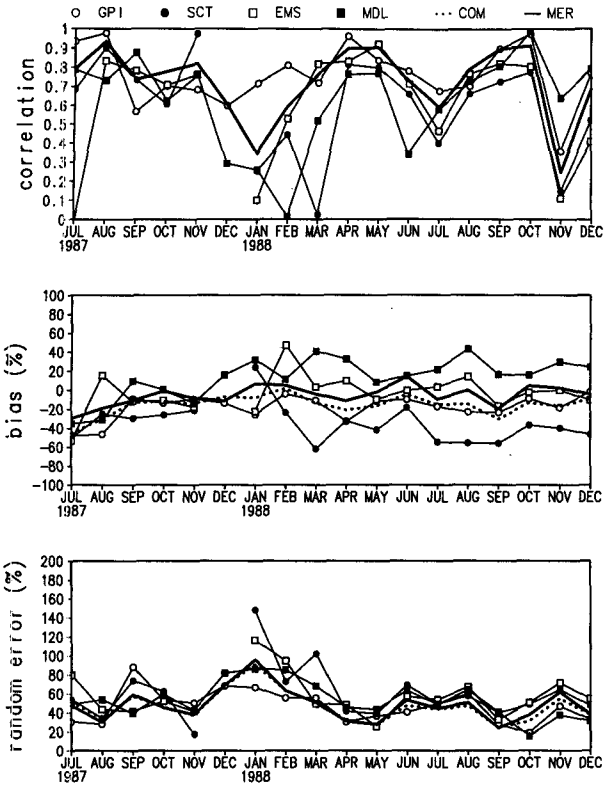

FIG. 4. Time series of correlation (top), bias (middle), and rms error (bottom) between the atoll gauge observations and the individual sources, the combined analysis, and the merged analysis over the unused atoll observations averaged over 2.5° × 2.5° grid areas in the tropical Pacific. GPI, SCT, EMS, MDL, COM, and MER denote the IR-based GPI, MW-scattering-based Grody estimates, MW-emission-based Chang estimates, ECMWF model predictions, the combined analysis, and the final merged analysis, respectively. The bias and rms error are plotted as a percentage of the verifying data; positive bias indicates an overestimate. Note that in the correlation plot, the combined and merged analyses are indistinguishable.

gorithm is used to blend the combined analysis with the gauge-based analysis and atoll observations. While the gauge-based analysis and atoll observations are clearly not completely unbiased, as discussed above, their biases are thought to be small, where sufficient observations are available, compared to those in the satellite estimates–model predictions and thus the combined analysis. The limited availability of gauge observations over ocean compared to land requires different bias removal methods for each.

Over land, where gauge observations are available to the GPCC analysis for more than one-half of the grid areas, the blending algorithm of Reynolds (1988) is used. Reynolds' algorithm blends the gauge-based analysis G and the combined analysis C into a blended analysis B by assuming that:

1) the relative distribution, or the "shape," of the blended analysis B satisfies Poisson's equation

$$\nabla^2 B = f, \tag{4}$$

where 2) the forcing term f in Eq. (4) is determined by the combined analysis C

$$f = \nabla^2 C, \tag{5}$$

3) and the boundary conditions are derived by assuming that the amplitude of the field B is determined by the gauge-based analysis G at grid areas with adequate measurement accuracy (anchor points):

$$B = G \quad \text{at anchor points.} \tag{6}$$

All of the three elements are reasonably applicable to the present situation. Poisson's equation has been applied frequently in the analysis of meteorological fields (Harris et al. 1966; Oort and Rasmusson 1971; Reynolds 1988). The similarity of the gradients of the combined analysis to actual areally averaged precipitation is strongly supported by the performance tests conducted in the previous section. Finally, the requirement for anchor points is satisfied by selecting those grid areas containing enough gauges. Schneider et al. (1993) and Xie and Arkin (1995) have shown that areal averages made from five or more gauges can provide monthly rainfall observation for most 2.5° latitude–longitude grid areas with an accuracy of 10%.

This blending procedure is limited to land areas where the GPCC gauge-based analysis is available.

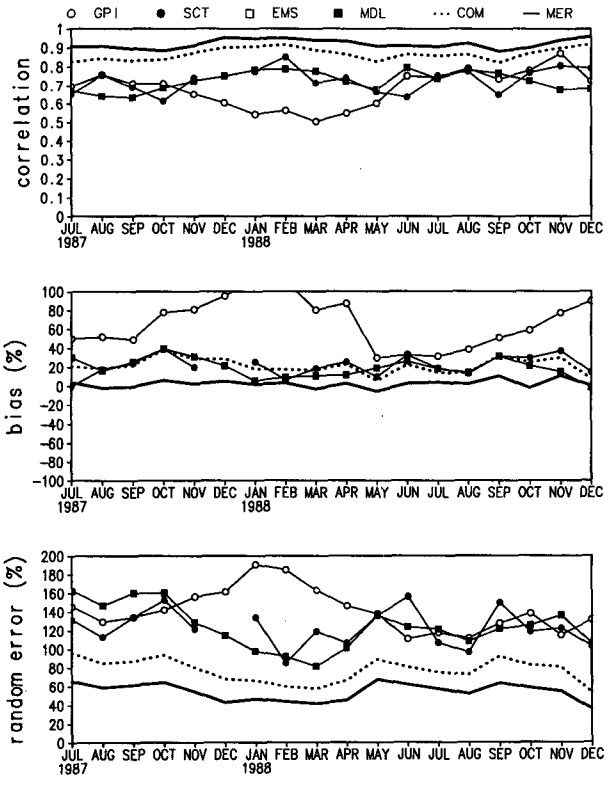

FIG. 5. As in Fig. 4 except that the statistics are computed using the withheld portion of the GPCC gauge-based analysis in the tropical land areas (40°S–40°N).

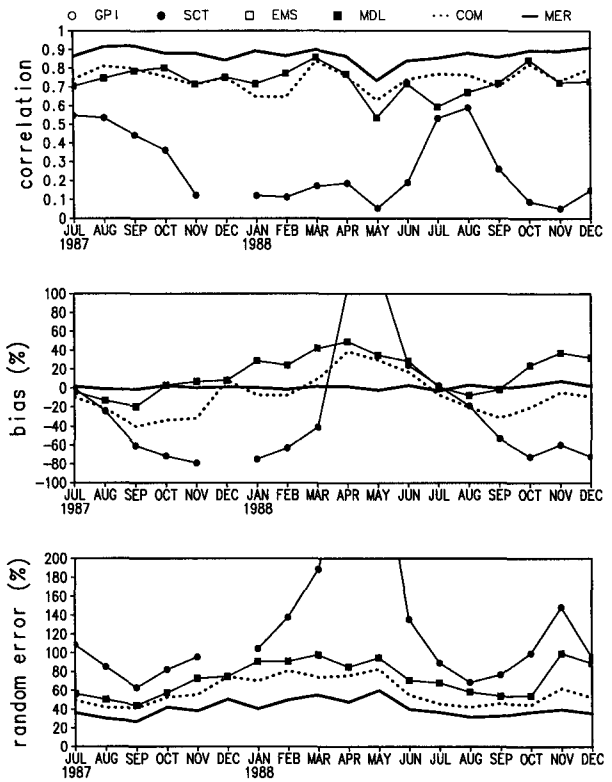

FIG. 6. As in Fig. 4 except that the statistics are computed using the withheld portion of the GPCC gauge-based analysis in the extratropical land areas (40°–90°S; 40°–90°N).

Thus, we define the blended analysis B at the coastal boundary as identical to the gauge analysis G regardless of the number of gauges used there:

$$B = G \quad \text{at external boundary.} \tag{7}$$

The blended analysis B over land is constructed by solving Eq. (4) numerically by relaxation with constraints imposed at internal (anchor points) and external (coastal) boundary grid areas (Richtmeyer and Morton 1967). The calculation procedure is repeated until the difference (residual) between two successive analyses is less than 0.01 mm day^{-1} for all of the grid areas over the target domain.

The advantage of this algorithm in the present application is its ability to retain the distribution information of the combined analysis while utilizing the amplitude information present in the gauge-based analysis. While the algorithm will generate a final product over land with bias smaller than that in the combined analysis, it will not necessarily remove all bias. Certainly any bias in the gauge-based analysis will remain in the merged analysis. Further, the process implicitly interpolates the bias between the gauge-based analysis and the combined analysis into regions between anchor points. In regions where the bias varies nonlinearly in space, the blending process cannot remove all the bias.

The blending procedure can be used only over land areas where a reasonable distribution of anchor points is available. Over oceanic areas, the only gauge observations widely available are the atoll gauge precipitation observations compiled by Morrissey and Greene (1991) over the tropical Pacific for each month. We use these observations to define the relative bias over the entire tropical ocean, defined as in section 3a. Since we have no useful observations for higher-latitude ocean regions, we assume that the relative bias decreases poleward from the tropical values at the seasonally moving tropical boundaries to zero at 60°S and 60°N and remains constant at zero poleward of 60°.

b. Tests with synthetic data

While the oceanic bias removal method is based on subjective assumptions and is therefore impossible to test without additional data, we can test the performance of the algorithm in blending the gauge-based and combined analyses over land areas, given varying coverages, biases, and random errors. As in the tests of the combining algorithm discussed in section 3b, these

TABLE 2. Bias (as a percentage of the validating data, with positive bias indicating an overestimate), rms error (again, as a percentage of the validating data values), and correlation of the several satellite estimates–model forecasts, as well as the combined (see section 3) and merged (see section 4) analyses, with the unused gauge-based analysis and atoll values. Validating data for the tropical ocean area are the unused (see text) atoll observations of Morrissey and Greene (1991), while over land areas they are the unused values from the GPCC gauge-based analysis.

Area	STAT	GPI	Grody	Chang	ECMWF	Combined	Merged
Tropical ocean	Bias (%)	19.7	−15.3	−4.4	9.9	−16.8	−6.4
	RMSE (%)	49.7	65.4	67.0	61.4	51.5	51.9
	Correlation	0.756	0.599	0.603	0.599	0.732	0.738
Tropical land	Bias (%)	7.1	20.7	—	18.3	20.5	2.1
(40°N–40°S)	RMSE (%)	147.1	122.5	—	123.7	77.0	54.3
	Correlation	0.666	0.727	—	0.714	0.862	0.920
Extratropical land	Bias (%)	—	−20.1	—	10.5	−9.5	0.8
	RMSE (%)	—	149.2	—	73.6	60.5	40.6
	Correlation	—	0.338	—	0.717	0.751	0.891

tests allow us to examine the behavior of the algorithm in controlled circumstances and to verify that it performs as we need it to.

Again, the target field is defined as the merged analysis for August 1987. Synthetic gauge-based and combined analyses are formed by defining their spatial coverages and then adding simplified but realistic bias and random error to the target field. The synthetic gauge field is assumed to be unbiased, while the coverage, which here represents the number of anchor points, and the random error vary from 5% to 50%. In the actual gauge-based analysis, the coverage depends upon the definition of anchor points; if five gauges are necessary, the coverage is typically 5%–10%, while if only a single gauge is required, the coverage is close to 50%. The random error of the gauge-based analysis is not well known because of the difficulty in finding validating datasets, but values of 10%–20% are considered reasonable. In the synthetic combined analyses, the coverage and the bias are assumed to be 100% and 5.0 mm/day, representative of the various satellite estimates, while the random error varies from 20% to 200% (Xie and Arkin 1995).

We apply the blending algorithm to a range of combinations of the synthetic gauge-based and combined analyses with varying coverages, biases, and random errors and compare the resulting blended analyses with the target field. The first series of tests uses a combined analysis with 80% random error, representing a field more accurate than any of the individual satellite estimates–model predictions but with significant residual bias, and synthetic gauge-based analyses with varying coverages and random errors. Results show that the bias (Fig. 7a) is reduced from 5 mm/day to less than 0.1 mm/day for coverage of anchor points greater than 10%–15% and random errors from 5%–50%. The relative random error (Fig. 7b) is nearly the same as that of the combined analysis for most combinations of gauge coverage and error, showing that the error in the merged analysis is not strongly affected by error in the gauge-based analysis. We next examine a series of blended analyses using synthetic gauge-based analyses with 30% coverage and varying random errors and synthetic combined analysis fields with varying random errors. Again, the bias of the merged analysis is effectively eliminated (from 5 mm/day to less than 0.05 mm/day) relative to that of the combined analysis, when the combined analysis has error less than 100% and the coverage of anchor points is 20% or greater (Fig. 8). Thus, in tests with synthetic data, the blending procedure is successful in removing the bias in the combined analysis without exaggerating its random error.

c. Validation

The blending algorithm requires anchor points where the gauge-based analysis is nearly free of bias. We use a threshold on the number of the gauges available in each 2.5° latitude–longitude grid area as the criterion to define the anchor points, because both the gauge-based analysis error for a grid area and the coverage of anchor points in the target domain are functions of the gauge number (Xie and Arkin 1995). The threshold chosen will clearly have a large impact on the coverage of anchor points, and so we constructed a series of merged analyses using thresholds ranging from one to five gauges per grid area to define anchor points. As in

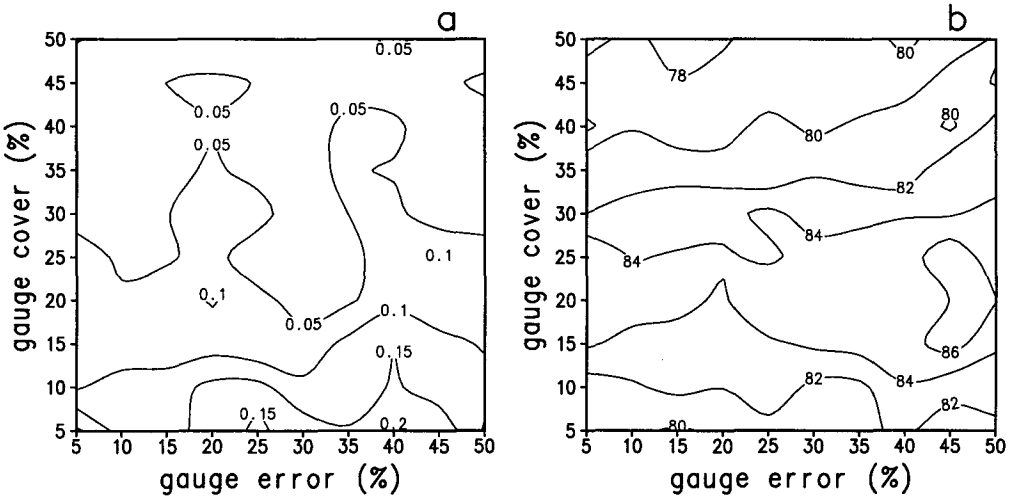

FIG. 7. Biases in millimeters per day (a) and relative rms errors in percent (b) between the target field (the merged analysis for August 1987) and the blended analyses obtained from synthetic combined analyses with bias of 5.0 mm/day and random error of 80% and synthetic gauge-based analyses with various coverages of anchor points and varying random errors.

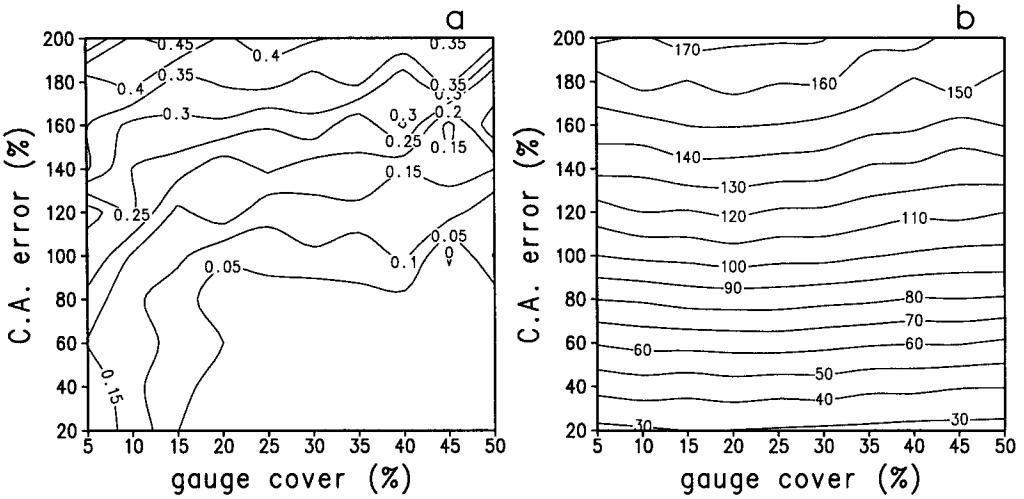

FIG. 8. Biases in millimeters per day (a) and relative rms errors in percent (b) between the target field (the merged analysis for August 1987) and the blended analyses obtained from synthetic combined analyses with bias of 5.0 mm day^{-1} and a range of random errors and synthetic gauge-based analyses with varying coverages of anchor points and a fixed random error of 30%.

section 3c, we first excluded a randomly chosen 25% of the grid areas in the gauge-based analysis so as to have unused, potentially independent, observations against which to compare our results.

Figure 9 shows the differences between the 18-month averages of the blended analyses obtained by defining anchor points as those with at least one and five gauges. The largest differences are found, as expected, in regions where gauge networks are relatively sparse, including portions of Africa and South America. Western North America and south-central Asia also exhibit substantial differences, while differences are less than 0.2 mm day^{-1} over land areas with relatively dense gauge networks, such as Europe and China.

The comparison between the blended analysis and the withheld grid areas of the gauge-based analysis for the 18-month period for tropical and extratropical areas shows that the blended analysis tends to exhibit higher correlations and smaller random errors as the number of gauges required to define anchor points decreases

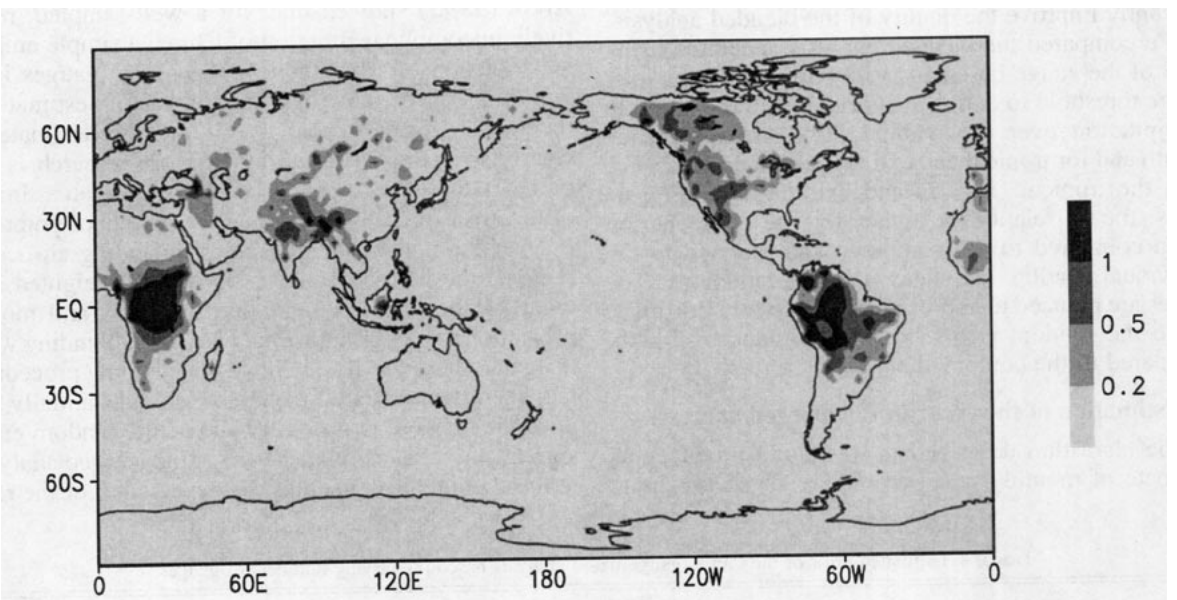

FIG. 9. Absolute differences (mm/day) between the 18-month means of the blended analyses constructed by defining the anchor grid areas as those with at least one and five gauges.

TABLE 3. Comparison of results between the GPCC and the blended analysis with different definitions of "anchor points."

Area	STAT	1	2	3	4	5
Tropical land	Bias (%)	2.1	6.3	8.9	13.9	14.8
	RMSE (%)	54.3	62.9	67.3	70.3	71.6
	Correlation	0.920	0.895	0.883	0.877	0.873
Extratropical land	Bias (%)	0.8	1.5	3.0	2.7	0.2
	RMSE (%)	0.6	43.9	45.8	48.2	50.0
	Correlation	0.891	0.872	0.859	0.847	0.837

for all land areas. In extratropical regions, the bias of the analysis is quite small for all definitions of anchor points. Nonnegligible biases, however, remain in the blended analyses when anchor points are defined as those with two or more gauges for tropical land areas where gauge networks are extremely sparse. This agrees with the results of the tests using synthetic data, which showed that the blending algorithm is unable to remove the bias effectively when the coverage of anchor points is less than 20%. Over tropical Africa and South America, most grid areas have zero to one gauge, and virtually none satisfies the five-gauge criterion. To ensure reasonable quality of the precipitation analyses over tropical land areas, and because differences in the quality resulting from different anchor point definitions are not so large for extratropical land areas, we have chosen here to define anchor grid areas as those with at least one gauge. As the GPCC processing progresses, more gauges will be available in such regions and the threshold for definition of anchor points may rise. As the role of the blending process is to reduce the bias, and since the bias of anchor points defined using a single gauge in each 2.5° × 2.5° area is probably larger than that obtained from using five gauges in the same area, we expect the availability of more gauges to significantly improve the quality of the blended analysis.

We compared the blended analysis generated using 75% of the gauge-based analysis grid areas and a one-gauge threshold to define anchor points to the monthly precipitation over the withheld grid areas for each month and for tropical and extratropical land areas. For both the tropical (Fig. 5) and extratropical (Fig. 6) areas, the correlation is higher for the entire period when compared to the combined analysis and to the individual satellite estimates–model predictions. The biases are reduced to approximately zero for both areas, while the random errors have been reduced slightly compared to the combined analysis.

5. Estimation of the error in the merged analysis

The algorithm described in this study produces an estimate of monthly mean areally averaged precipitation for areas of 2.5° × 2.5° latitude–longitude over the globe. In order to ensure appropriate and successful application of the merged analysis, an estimate of the error or uncertainty of the analysis is required (WCRP 1993). The definition of this error, however, requires caution. Because of the random nature of the error, it is not possible to specify the exact error in the merged analysis for a given grid area and month. Instead, the error is defined as the expectation (or the average) of the error that might be found in the merged analysis over specified grid areas under certain conditions.

As described in section 4, all grid areas can be divided into two types, anchor points and others, according to the methods used to define the merged analysis. Different methods are used to estimate the error for each. At the anchor points, the merged analysis is defined as equal to the value of the GPCC gauge-based analysis at that point. The GPCC analysis is constructed for each grid area by interpolating the station observations available within and near the target area. The error found in such an analysis is a complicated function of precipitation variability, local gauge distribution, topography, and many other parameters (Schneider et al. 1993; Rudolf et al. 1994). However, Xie and Arkin (1995) showed that, for a well-sampled, relatively uncomplicated region of China, a simple empirical function of the number of available gauges in a 2.5° × 2.5° grid area provides a satisfactory estimate of the relative error (Table 4). While this estimate is clearly oversimplified and much more research is required, we use this function here to provide an estimate of the error of the blended analysis at anchor points.

Over the nonanchor grid areas, including all ocean regions, the merged analysis value is a weighted average of the individual satellite estimates and model predictions, with an adjustment based on blending with the gauge-based analysis. Since the blending procedure has been demonstrated to be able to substantially reduce the bias but is unable to reduce the random error significantly, the estimated error of the merged analysis at these points is defined as the expectation of the ran-

TABLE 4. Estimated error of the GPCC gauge-based analysis based on varying numbers of gauges.

Gauge number	1	2	3	4	5	6	7	8	9	⩾10
Error (%)	30	25	20	15	12	10	8	7	6	5

dom error of the combined analysis, calculated from Eq. (3) from the random errors for the individual sources.

This method of estimating the error of the merged analysis can be checked by comparing it to direct calculation of root-mean-square error in a region with a relatively dense network of gauge observations. We have made this comparison for the land area of China (20°–40°N, 100°–125°E) using grid areas with at least five gauges (rather than one) as anchor points in the blending procedure so as to have enough nonanchor grid areas to define the error estimate and to compare with the gauge observations. Since the error estimated for a grid area is an estimate of the average error expected for grid areas under similar conditions, the estimated error value for each grid area is compared to the root-mean-square difference between the merged analysis and the GPCC gauge-based analysis over the nonanchor grid areas in a 7 × 7 array of grid areas centered at the target point. Figure 10 shows the scatter plot comparing the estimated and calculated errors. Although substantial scatter is seen, especially for larger errors, the results are encouraging considering the large number of assumptions that went into the process. The error estimated from the errors of the satellite estimates–model predictions agrees quite well with that calculated from the direct comparison of the merged analysis with the GPCC analysis. The correlation between the theoretical and the calculated errors is 0.878. While this is encouraging, one must remember that this region is one of those that Xie and Arkin (1995) used to estimate the errors of some of the satellite estimates and that the gauge-based analysis is of particularly high quality here because of the density of gauges available. Thus, the results here are probably an upper bound on the accuracy of the estimated error of the merged analysis.

At this stage, we are unable to examine the accuracy of the error estimation over oceanic areas, where error structures for the individual sources are based principally on empirical comparisons with small sets of observations and on somewhat arbitrary extrapolation of those results. Additional observational data are needed to improve the error definitions for each individual source and thereby to refine the merged analysis.

6. Application of the merging algorithm

The results of the performance tests conducted for both the combining and blending procedures show the merging algorithm to be successful in reducing random errors and biases compared to the contributing components. The algorithm was therefore used to construct monthly analyses of global precipitation for the 18-month period from July 1987 to December 1988 by merging the GPCC gauge-based analysis, the GPI, Grody, and Chang estimates, and the ECMWF numerical model predictions.

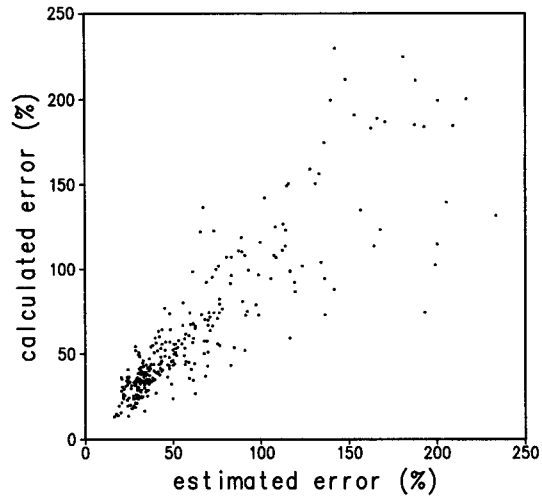

FIG. 10. Scatterplot of the relative random errors over China (20°–40°N, 100°–125°E) as calculated through theoretical error definition of the maximum likelihood estimation and by comparison with the GPCC gauge data.

Shown in Fig. 11 are the distributions of estimated precipitation for August 1987 using the GPI, Grody, and Chang estimates, and the ECMWF model predictions. None of the four individual sources provides full global coverage with acceptable quality. As has been noted previously (Arkin and Meisner 1987), the GPI exhibits unrealistically high estimates over tropical continental regions and extratropical ocean areas in the Southern Hemisphere, as well as latitudinally limited coverage. The Grody algorithm appears to underestimate precipitation over the Southern Ocean and contains some erroneous values resulting from underlying ice over the Arctic, and the Chang estimates are available only over oceans and contain relatively large noise caused by the low resolution and infrequent sampling of the instrument. The ECMWF predictions depict the ITCZ and South Pacific convergence zone (SPCZ) as somewhat broader than any of the observation-based sources.

Figure 12 presents the combined analysis, the GPCC gauge-based analysis, the merged analysis, and the relative error for August 1987. The merged analysis appears to take appropriate advantage of the strengths of the individual sources. It has a generally smoother distribution than the sources based on SSM/I observations. It is identical to the GPCC analysis at most grid areas over the United States, China, and Europe, where dense gauge networks are available. Over other continental regions, including in particular Africa and South America, where gauge observations are more sparse, the merged analysis derives its spatial distribution from the satellite estimates and model predictions, while its amplitude is controlled by the GPCC analysis. Also shown in Fig. 12 is the distribution of the estimated

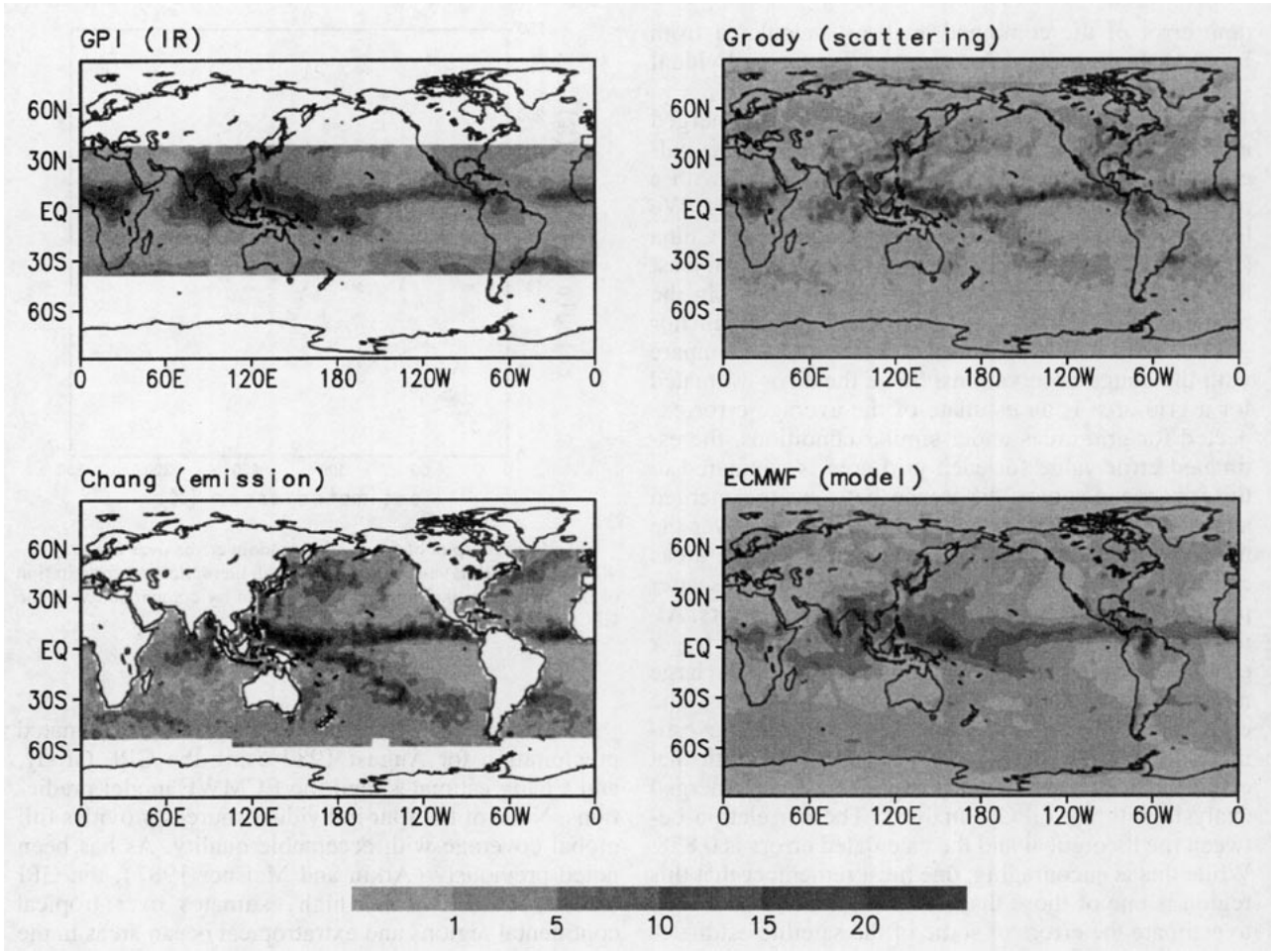

FIG. 11. Global precipitation distributions (mm/day) for August 1987 from the GPI, Grody, and Chang satellite-derived estimates and the ECMWF model predictions.

random error of the merged analysis. Relatively small errors are observed over tropical oceanic areas and populated land areas, while relatively large errors are found over coastal grid areas, where the Chang estimates are excluded from the combining procedure and the merged analysis is identical to the GPCC analysis regardless of the number of observations available to it. Note that this estimate of the random error of the merged analysis excludes any residual bias errors in the analysis.

The 18-month mean of the merged analysis (Fig. 13) is compared with the long-term mean precipitation climatologies as published by Legates-Willmott (1990, hereafter referred to as L-W and Jaeger (1976, hereafter referred to as J). In the computation of the L-W and Jaeger fields shown in Fig. 13, the months from July through December receive twice the weight of the other months to enable an appropriate comparison. Generally speaking, similar large-scale spatial distributions are found in the climatologies and in the merged analysis, with rainbands associated with the ITCZ and SPCZ over the Tropics and with the storm tracks over northwest Pacific and Atlantic Oceans as well as over the Southern Ocean. Significant differences are seen in the central and eastern Pacific ITCZ, with particularly large values extending quite far to the south in L-W near 140°W. Jaeger shows wider and smoother distributions for the ITCZ and SPCZ, while the merged analysis is intermediate. A detailed analysis of these features, particularly the large values in the eastern Pacific in L-W, can be found in Janowiak et al. (1995).

Since analyses of global precipitation are often used as a tool to verify atmospheric general circulation models (WCRP 1993), a model-independent version of the merged analysis is created by omitting the ECMWF predictions and using only the observation-based data sources. Also shown in Fig. 13 is the distribution of the 18-month mean precipitation for this model-independent version of the merged analyses. Major differences

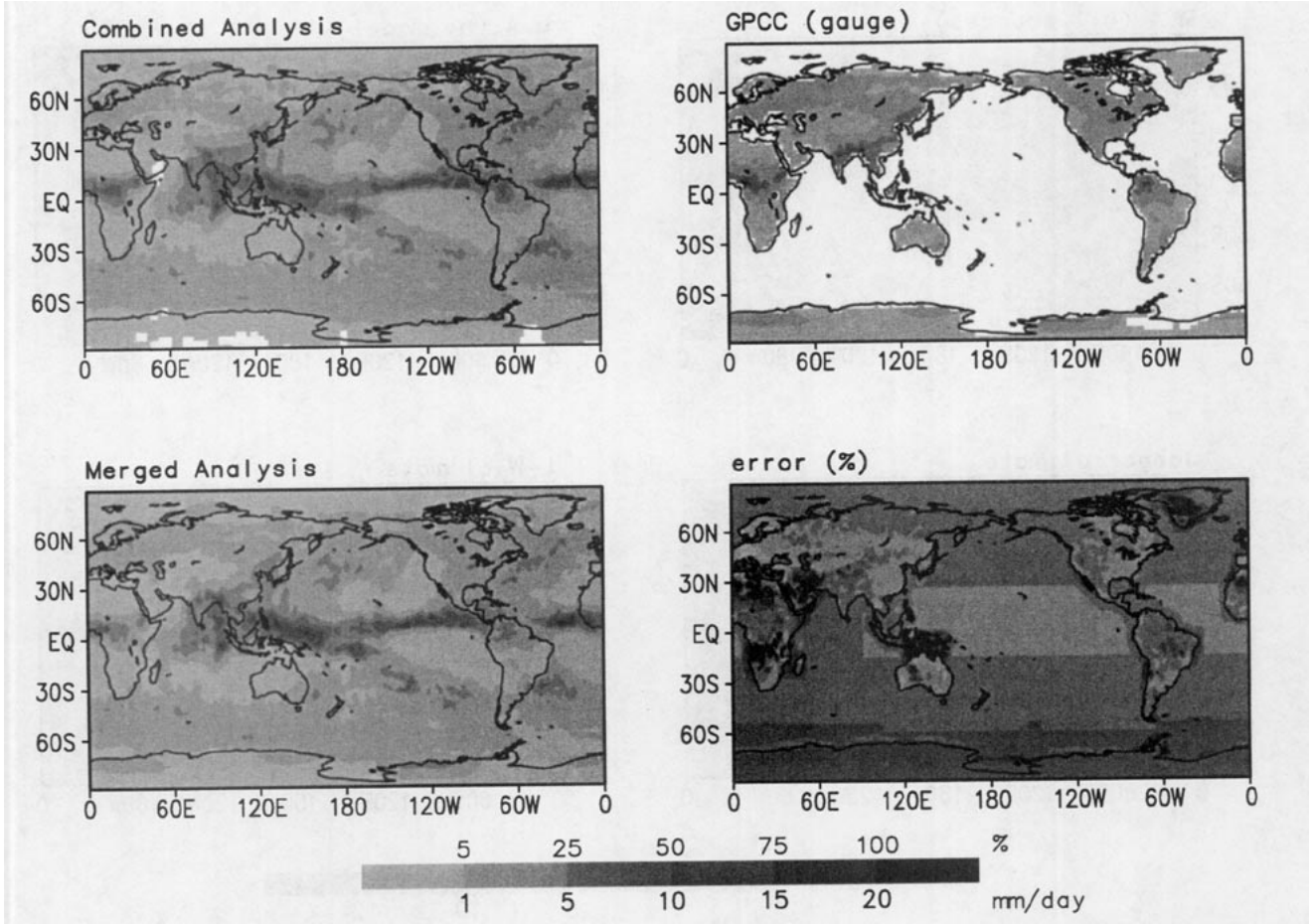

FIG. 12. Global precipitation distributions (mm/day) for August 1987 from the combined analysis, the GPCC gauge-based analysis and the merged analysis, along with the estimated error of the merged analysis in percent. Note that the scale for the estimated error differs from that for the three precipitation maps by a factor of five.

between the original and the model-independent versions of the merged analyses are observed over high latitudes, especially over the Southern Ocean, where the only observational data available are the MW scattering-based Grody estimates. Over tropical and subtropical regions, where the observation-based sources exhibit relatively high quality, the model-independent version is nearly identical to the version using the model predictions.

Time series of global mean precipitation computed from the two versions of the merged analysis, the ECMWF model predictions, L-W, and J for the 18-month period are shown in Fig. 14. The two versions of the merged analysis exhibit similar patterns of temporal variation with only minor differences in amplitudes resulting from the inclusion of the model data. Both versions agree closely in amplitude with the Jaeger climatology. The global averages of the ECMWF model predictions exhibit consistently larger values of mean precipitation than the merged analyses, while the amplitude of the L-W climatology agrees with Jaeger and the merged analyses from March through August but is much higher during the remainder of the year.

7. Summary and conclusions

An algorithm has been developed to construct monthly analyses of global precipitation by merging five separate data sources, including gauge observations, three kinds of satellite estimates, and numerical weather forecast model predictions. The algorithm uses successive steps to reduce the random errors of the contributing components and then to reduce their biases. This algorithm is used to produce monthly analyses of global precipitation for the 18-month period from July 1987 to December 1988. The distribution and amplitude of large-scale spatial patterns of precipitation in the merged analysis are generally consistent with earlier observational studies. While the quality of the merged analysis is uncertain over oceanic regions,

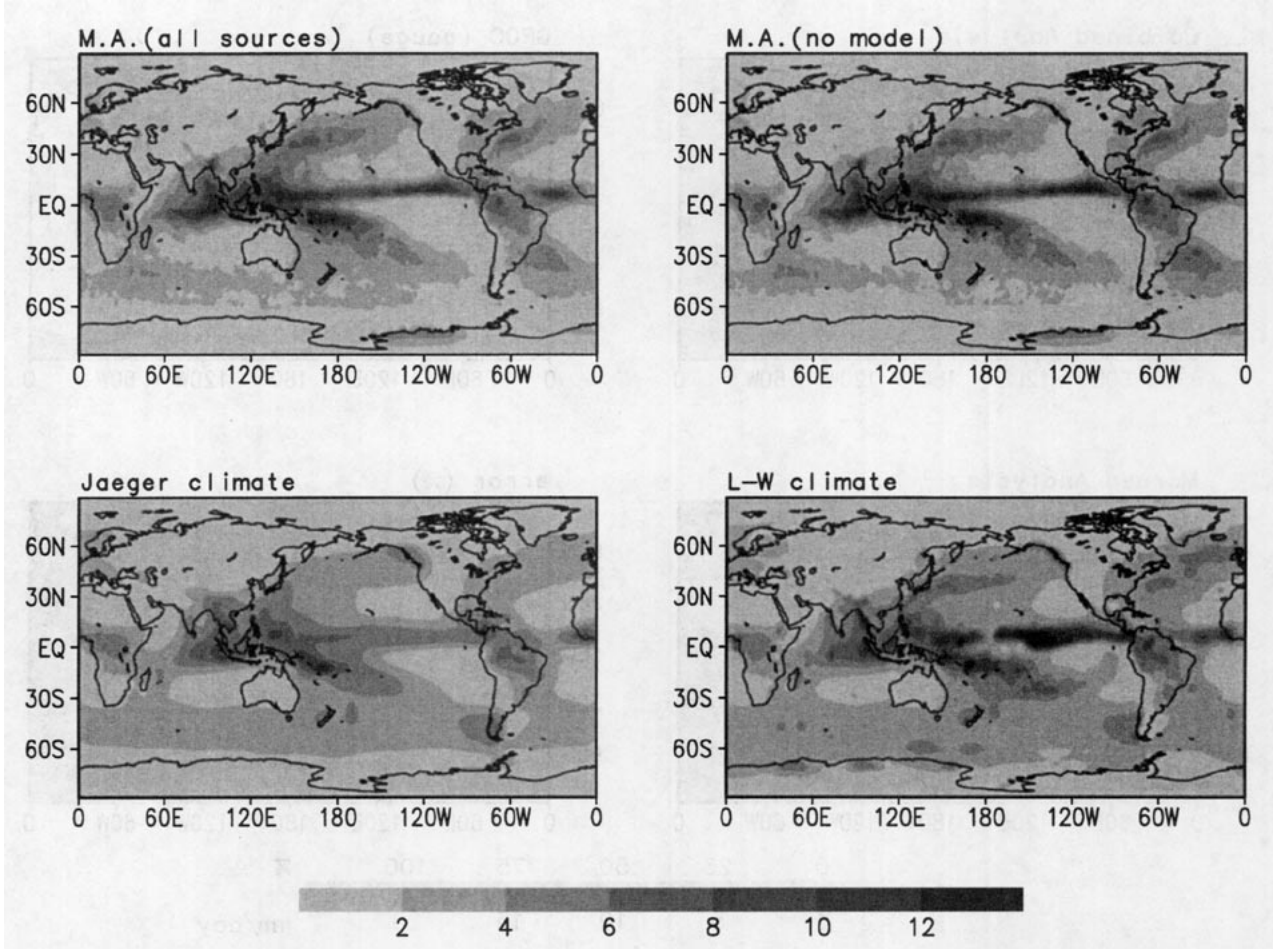

FIG. 13. The 18-month mean distributions (mm/day) of the merged analyses obtained by using all sources and using sources without model predictions. Long-term averages of Jaeger (1976) and of Legates and Willmott (1990) are also plotted for comparison.

where both the combining and blending steps rely strongly on empirical findings and subjective extrapolation and where little or no additional observational data are available for verification, the merging algorithm has demonstrated the capacity to provide complete global coverage of monthly precipitation with substantially improved quality compared to the individual sources.

A similar algorithm has been developed by Huffman et al. (1995). Both the algorithm described here and that of Huffman et al. compute global gridded fields of monthly precipitation from a weighted average of a mix of satellite-derived estimates, model forecasts, and a gauge-based analysis. There are significant differences between the two algorithms, involving the reduction of bias in the final product, the use of model predictions, and the definition of the error structures of the components used in the analysis. However, we believe that both algorithms produce useful depictions of global precipitation on monthly timescales. Development of both our algorithm and that of Huffman et al. is continuing.

In particular, more work is needed to improve the quality of the individual data sources and to obtain better knowledge of the error structures, especially over the oceans. Since the final quality of the merged analysis is dominated by the quality of the individual sources, improvements in the individual sources are essential, particularly over middle and high latitudes. Improved knowledge of the random and systematic error structures of the various components is crucial to ensure successful execution of the combining and blending procedures, especially over oceanic areas where empirical results and subjective assumptions are most strongly relied upon. Implementation of the Tropical Rainfall Measuring Mission (TRMM; Simpson et al. 1988) and additional gauge observations from the Tropical Atmosphere–Ocean (TAO) array of moored buoys (McPhaden and Milburn 1992) are expected to provide precipitation observations from which error

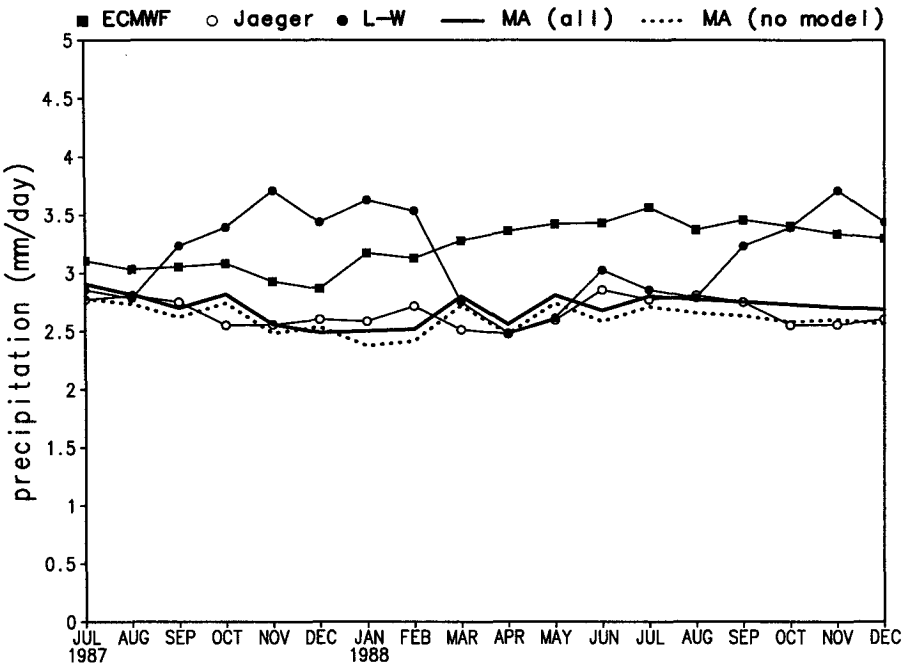

FIG. 14. Time series of global mean precipitation (mm/day) as obtained from ECMWF model predictions, the merged analyses using all sources, and the merged analyses excluding model predictions. Long-term averages of Jaeger (1976) and Legates and Willmott (1990) are plotted as well for comparison.

structures of the individual sources can be estimated more accurately over oceans. Finally, enhancements to the algorithm to make use of the horizontal correlations present in the various estimates used are required.

Acknowledgments. The authors would like to thank J. Janowiak of the Climate Analysis Center and R. Joyce of Research and Data System, Inc., for advice and technical assistance. The MW-based Grody and Chang estimates were supplied by Dr. N. Grody and R. Ferraro of NOAA/NESDIS and Dr. A. Chang of NASA/GSFC, while the GPCC gauge analyses and the ECMWF model predictions were provided by the WCRP Global Precipitation Climatology Centre in Germany. Thanks are extended to Dr. A. Gruber, Dr. E. Rasmusson, and C. Ropelewski for valuable discussions throughout the research. Reviews of an early version of the manuscript by Drs. E. Kalnay, S. K. Yang, H.-B. Chen, D. Martin, F.-Z. Weng, and Profs. W. F. Krajewski, D.-R. Lu, and J.-L. Liu were most helpful. We are grateful to two anonymous reviewers and to our editor, Dr. James Coakley, for helpful suggestions and the opportunity to improve upon the version originally submitted. Most of the work was done while the first author was a UCAR visiting scientist at the National Meteorological Center of NOAA.

REFERENCES

Adler, R. F., P. R. Keehn, and I. M. Hakkainen, 1993: Estimation of monthly rainfall over Japan and surrounding waters from a combination of low-orbit microwave and geosynchronous IR data. *J. Appl. Meteor.*, **32,** 335–356.

——, G. J. Huffman, and P. R. Keehn, 1994: Global tropical rain estimation from microwave-adjusted geosynchronous IR data. *Remote Sens. Rev.*, **11,** 125–152.

Arkin, P. A., 1979: The relationship between fractional coverage of high cloud and rainfall accumulations during GATE over the B-scale array. *Mon. Wea. Rev.*, **107,** 1382–1387.

——, and B. N. Meisner, 1987: The relationship between large-scale convective rainfall and cold cloud over the western hemisphere during 1982–1984. *Mon. Wea. Rev.*, **115,** 51–74.

——, and P. E. Ardanuy, 1989: Estimating climatic-scale precipitation from space: A review. *J. Climate,* **2,** 1229–1238.

——, and P. Xie, 1994: The Global Precipitation Climatology Project: First Algorithm Intercomparison Project. *Bull. Amer. Meteor. Soc.,* **75,** 401–419.

——, R. Joyce, and J. E. Janowiak, 1994: IR techniques: GOES Precipitation Index. *Remote Sens. Rev.*, **11,** 107–124.

Arpe, K., 1991: The hydrological cycle in the ECMWF short-range forecasts. *Dyn. Atmos. Oceans,* **16,** 33–60.

Barrett, E. C., and D. W. Martin, 1981: *The Use of Satellite Data in Rainfall Monitoring.* Academic Press, 340 pp.

——, J. Dodge, M. Goodman, J. Janowiak, and E. Smith, 1994: The First WetNet Intercomparison Project (PIP-1). *Remote Sens. Rev.*, **11,** 49–60.

Bell, T. L., 1987: A space-time stochastic model of rainfall for satellite remote-sensing studies. *J. Geophys. Res.*, **92D,** 9615–9630.

Browning, K. A., 1979: The FRONTIERS plan: A strategy for using radar and satellite imagery for very-short-range precipitation forecasting. *Meteor. Mag.*, **108,** 161–184.

Chiu, L. S., A. T. C. Chang, and J. E. Janowiak, 1993: Comparison of monthly rain rates derived from GPI and SSM/I using probability distribution function. *J. Appl. Meteor.*, **32,** 323–334.

Conway, B. J., 1987: FRONTIERS: An operational system for nowcasting precipitation. *Proc. Symp. Mesoscale Analysis and Forecasting,* Vancouver, BC, Canada, ESA SP-282, 233–238.

Daley, R., 1991: *Atmospheric Data Analysis.* Cambridge University Press, 457 pp.

Dodge. J., 1994: The WetNet project. *Remote Sens. Rev.,* **11,** 5–21.

Ferraro, R. R., N. C. Grody, and G. F. Marks, 1994: Effects of surface conditions on rain identification using SSM/I. *Remote Sens. Rev.,* **11,** 195–209.

GPCC, 1992: Monthly precipitation estimates based on gauge measurements on the continents for the year 1987 (preliminary results and future requirements). World Climate Research Programme and Deutscher Wetterdienst.

——, 1993: Global area-mean monthly precipitation totals for the year 1988 (preliminary estimates, derived from rain-gauge measurements, satellite observations and numerical weather prediction results). Deutscher Wetterdienst.

Grody, N. C., 1991: Classification of snow cover and precipitation using the Special Sensor Microwave Imager. *J. Geophys. Res.,* **96,** 7423–7435.

Harris, R. G., A. Thomasell, and J. G. Welsh, 1966: Studies of techniques for the analysis and prediction of temperature in the ocean, Part III. Interim Rept., prepared by Travelers Research Center, Inc., for the U.S. Naval Oceanographic Office, Contract N62306-1675, 97 pp.

Huffman, G. J., R. F. Adler, B. R. Rudolf, U. Schneider, and P. R. Keehn, 1995: Global precipitation estimates based on a technique for combining satellite-based estimates, raingauge analysis, and NWP model precipitation information. *J. Climate,* **8,** 1284–1295.

Jaeger, L., 1976: Monatskarten des Niederschlags fur die ganze Erde. *Ber. Dtsch. Wetterdienstes,* 139 (Band 18), 33 pp. and plates.

Janowiak, J. E., 1992: Tropical rainfall: A comparison of satellite-derived rainfall estimates with model precipitation forecasts, climatologies, and observations. *Mon. Wea. Rev.,* **120,** 448–462.

——, P. A. Arkin, P. Xie, M. M. Morrissey, and D. R. Legates, 1995: An examination of the East Pacific ITCZ Rainfall Distribution. *J. Climate,* **8,** 2810–2823.

Krajewski, W. F., 1987: Cokriging radar-rainfall and rain gage data. *J. Geophys. Res.,* **92,** 9571–9580.

——, 1992: Methods of merging multisensor rainfall observations: An outlook. *GPCP Workshop,* Koblenz, Germany, WCRP.

Legates, D. R., and C. J. Willmott, 1990: Mean seasonal and spatial variability in gage-corrected, global precipitation. *Int. J. Climate,* **10,** 111–127.

McPhaden, M. J., and H. B. Milburn, 1992: Moored precipitation estimates for TOGA. *TOGA Notes,* **7,** 1–5.

Morrissey, M. L., and J. S. Greene, 1991: The Pacific atoll raingage data set. Tech. Rep. Univ. Hawaii, Manoa, Honolulu, Hawaii.

——, and ——, 1993: Comparison of two satellite-based rainfall algorithms using atoll raingage data. *J. Appl. Meteor.,* **32,** 411–425.

Negri, A. J., and R. F. Adler, 1993: An intercomparison of three satellite infrared rainfall techniques over Japan and surrounding waters. *J. Appl. Meteor.,* **32,** 357–373.

Oort, A. H., and E. M. Rasmusson, 1971: *Atmospheric Circulation Statistics.* NOAA Prof. Paper No. 5, 323 pp. [Available from U.S. Govt. Printing Office, Washington, D.C., 20402, stock No. 0317-00450.]

Peixoto, J. P., and A. H. Oort, 1991: *Physics of Climate.* Amer. Inst. of Phys., 520 pp.

Reynolds, R. W., 1988: A real-time global sea surface temperature analysis. *J. Climate,* **1,** 75–86.

Richards, F., and P. A. Arkin, 1981: On the relationship between satellite-observed cloud cover and precipitation. *Mon. Wea. Rev.,* **109,** 1081–1093.

Richtmeyer, R. D., and K. W. Morton, 1967: *Difference Methods for Initial-Value Problems.* 2d ed., Interscience, 405 pp.

Rudolf, B., H. Hauschild, W. Rueth, and U. Schneider, 1994: Terrestrail precipitation analysis: Operational method and required density of point measurements. *NATO ASI Series,* **I26,** 173–186.

Schneider, U., B. Rudolf, and W. Ruth, 1993: The spatial sampling error of areal mean monthly precipitation totals analyzed from gauge measurements. *Fourth Int. Conf. on Precipitation,* Iowa City, IA, 80–82.

Sevruk, B., 1982: Methods of correction for systematic error in point precipitation measurement for operational use. WMO Oper. Hydro. Rep. 21, World Meteor. Org.,

Simpson, J., R. F. Adler, and G. R. North, 1988: A proposed tropical rainfall measuring mission. *Bull. Amer. Meteor. Soc.,* **69,** 278–295.

Takemura, Y., K. Takase, and Y. Makihara, 1984: Operational precipitation observation system using digital radar and rain gauges. *Proc. Nowcasting-II Symposium,* Norkoping, Sweden, ESA SP-208.

Waymire, E., V. K. Gupta, and I. Rodriguez-Iturbe, 1984: A spectral theory of rainfall intensity at the meso-β scale. *Water Resour. Res.,* **20,** 1453–1465.

Wilheit, T. J., A. T. C. Chang, and L. S. Chiu, 1991: Retrieval of the monthly rainfall indices from microwave radiometric measurements using probability distribution functions. *J. Atmos. Oceanic Technol.,* **8,** 118–136.

World Climate Research Programme, 1993: Global Observations, analyses and simulation of precipitation. WCRP-78, WMO/TD-No. 544, 136 pp.

Xie, P., and P. A. Arkin, 1995: An intercomparison of gauge observations and satellite estimates of monthly precipitation. *J. Appl. Meteor.,* **34,** 1143–1160.